LETTERS

Spatial cooperativity in soft glassy flows

J. Goyon[1], A. Colin[1], G. Ovarlez[2], A. Ajdari[3] & L. Bocquet[4,5]

Amorphous glassy materials of diverse nature—concentrated emulsions, granular materials, pastes, molecular glasses—display complex flow properties, intermediate between solid and liquid, which are at the root of their use in many applications[1–3]. A general feature of such systems, well documented yet not really understood, is the strongly nonlinear nature of the flow rule relating stresses and strain rates[4,5]. Here we use a microfluidic velocimetry technique to characterize the flow of thin layers of concentrated emulsions, confined in gaps of different thicknesses by surfaces of different roughnesses. We find evidence for finite-size effects in the flow behaviour and the absence of an intrinsic local flow rule. In contrast to the classical nonlinearities of the rheological behaviour of amorphous materials, we show that a rather simple non-local flow rule can account for all the velocity profiles. This non-locality of the dynamics is quantified by a length, characteristic of cooperativity within the flow at these scales, that is unobservable in the liquid state (lower emulsion concentrations) and that increases with concentration in the jammed state. Beyond its practical importance for applications involving thin layers (for example, coatings), these non-locality and cooperativity effects have parallels in the behaviour of other glassy, jammed and granular systems, suggesting a possible fundamental universality.

Glasses and jammed matter are at the heart of many challenging questions in condensed matter physics. The glass transition and the physical and mechanical properties of materials in the glassy or jammed state—from granular materials to dense colloidal suspensions—remain a puzzle to a large extent[2–8]. The transition itself is characterized by a dramatic slowing down of the system, associated with a dynamical arrest of the microscopic structure[3]. Although a large amount of work has been dedicated in recent years to demonstrating and characterizing dynamical heterogeneities in granular, glassy and glass-forming materials[9–16], the question of whether and how these dynamical heterogeneities influence the flow behaviour remains[17–19]. Indeed, one expects that such cooperative effects, which are in essence dynamical processes, should manifest themselves in the flow dynamics of jammed materials. This question is essential from the perspective of both fundamental science and applications: flows of jammed and glassy materials and glassy films are ubiquitous in nature and industry—for example, in granular flows, coatings with thin polymer films, lubrication processes in solid friction, in the food and cosmetic industries, and even in pedestrian dynamics[20].

In the present work, we aim to develop a constitutive law governing flows of jammed materials. We take advantage of a local velocity measurement technique to follow the local flow behaviour of a film of a confined soft glassy material (here a concentrated emulsion). We demonstrate the existence of finite-size effects in the flow dynamics that cannot be comprehended within our current understanding of the behaviour of fluids exhibiting yield properties.

To this end, we probe as sketched in Fig. 1 the flow of a jammed emulsion in various geometries and confinements: shear or pressure driven planar flow, in a wide gap Couette cell (centimetric gap) or a narrow microchannel (from tens to hundreds of micrometres in width). The emulsion is made of silicone droplets (~6.5 μm in diameter) in an index-matched glycerine–water mixture (Supplementary Methods). We are specifically interested in the local flow curves of the material, which relate the local shear stress σ to the local shear rate $\dot{\gamma}$ (Fig. 1c, d). Such curves can be constructed from the velocity profiles measured in the jammed emulsion in both geometries using local velocimetry techniques (Supplementary Methods; Fig. 1c, d insets). Indeed, in both geometries the stress distribution is known from mechanical equilibrium: $\sigma(R) = \Gamma/(2\pi HR^2)$ at a position R in the Couette cell (of height H) under a torque Γ; and $\sigma(z) = (\Delta P/L)[z-(w/2)]$ at a position $z-(w/2)$ from the centreline of the microchannel, under an applied pressure drop ΔP between the two ends of the channel of length L (ref. 21). Local shear rates $\dot{\gamma}$ are deduced directly from the velocity profiles. As shown in Fig. 1c, d, the local flow curves exhibit very different behaviours depending on the confinement of the material. In the wide gap Couette cell, all local flow curves obtained for different torques show a perfect superposition (Fig. 1c). The flow curve is furthermore well described by a classical Herschel-Bulkley model, $\sigma = \sigma_0 + A\dot{\gamma}^{1/2}$, with σ_0 a 'dynamical' yield stress and A a material constant. On the other hand, in the narrow microchannels, data for different pressure drops ΔP are scattered in the whole figure and do not collapse on a single rheological curve (Fig. 1d; see also Supplementary Fig. 4). Accordingly, whereas a single Herschel–Bulkley model accounts perfectly for all the velocity profiles in the wide gap Couette cell (Fig. 1c inset), such is not the case for the narrow microchannels (Supplementary Fig. 8). Furthermore, below the jamming point, $\phi < \phi_c$ (with ϕ the volume fraction and ϕ_c its value at jamming), the local Herschel–Bulkley rheological model is fully able to reproduce the flow behaviour, even in narrow channels (Supplementary Fig. 3).

In summary, a key feature emerges from the experimental data: in the jammed state, $\phi > \phi_c$, there is no universal local relationship between stress and shear rate. The occurrence of finite-size effects in the flow properties of the jammed emulsion in narrow microchannels, and their absence in a wide geometry, point to the existence of extended spatial correlations, the effects of which increase as the volume of material decreases. As a further confirmation of this point, the overall shape of the velocity profiles, for the same wall shear stress, is shown to vary with the thickness of the channel (Fig. 2). Rougher surfaces are shown to induce higher shear rates for the same confinement and shear stress at the wall.

We did not find any evidence that the above results stem from a coupling to a structural change of the emulsion itself: we checked that neither the size distribution of the droplets, nor their shape, was affected by the flow. Moreover, in all geometries no variation of local droplet concentration, such as depletion or local ordering at the confining surfaces, was measured within the gap up to the experimental uncertainty of ~1% in the volume fraction. This rules out

[1]LOF, Université Bordeaux 1, UMR CNRS-Rhodia-Bordeaux 1 5258, 33608 Pessac cedex, France. [2]Institut Navier, Université Paris Est, LMSGC, 77420 Champs sur Marne, France. [3]Gulliver, UMR CNRS – ESPCI 7083, 75005 Paris, France. [4]Laboratoire PMCN, Université Lyon 1, Université de Lyon, UMR CNRS 5586, 69622 Villeurbanne, France. [5]Physics Department, Technical University Munich, 85748 Garching, Germany.

density variations as the origin of non-local effects in the rheology (see Supplementary Fig. 10 and discussion in the legend). Such boundary effects on particle density have been reported in other disordered systems, such as granular materials and colloidal glasses[19,22], and their absence in the present case may be attributed to the relative softness of individual particles—which minimizes dilatancy effects—and the rather large polydispersity of the emulsions. We emphasize that the volume fraction of the emulsions, here typically 75–85%, is well above the jamming threshold (~64%), so that one does expect a relative insensitivity to local density variations. Altogether, our results suggest that the flow does not couple to a structural order parameter, so that non-local effects are 'intrinsic' to the rheology of the jammed emulsion, in line with similar observations in numerical simulations for glassy flows[17].

On the basis of these experimental facts, we now propose a theoretical framework able to rationalize these finite-size effects in the rheological behaviour. In concentrated emulsions, and more generally in soft glasses, flow occurs via a succession of reversible elastic deformations and local irreversible plastic rearrangements associated with a microscopic yield stress[23–26]. These localized plastic events induce a non-local, long ranged, elastic relaxation of the stress over the system. The number of plastic rearrangements per unit time, ν, plays the role of an inverse relaxation time and therefore controls the flow and relaxation of the material: a higher rate is associated with a more fluid system. Up to an elastic modulus G, the rate of rearrangements ν is equivalent to a 'fluidity', f, defined as $\sigma = (1/f)\dot{\gamma}$, a quantity that has been used in recent studies to characterize the rheology of fluids exhibiting yield properties[25]. In the absence of any non-local effect, the fluidity would reduce to its bulk value, $f_{\mathrm{bulk}} = \dot{\gamma}/\sigma_{\mathrm{bulk}}$ (note that for the Herschel-Bulkley expression reported above, $f_{\mathrm{bulk}} \propto \dot{\gamma}$ in the quasistatic limit, as $\sigma \to \sigma_0$.) Now, owing to the non-local elastic relaxation of plastic rearrangements ('dynamical cooperativity')[24,26], a dynamically active region will induce agitation of its neighbours, and thus a higher rate of plastic rearrangements (and vice versa for a dynamically quiescent region). This suggests that non-local effects will occur for the rearrangement rates and consequently for the fluidity, f. In order to capture this physical picture, we assume that the local fluidity, $f(z)$, obeys a non-local equation in the steady state:

$$f(z) = f_{\mathrm{bulk}} + \xi^2 \frac{\partial^2 f(z)}{\partial^2 z} \qquad (1)$$

In this equation, the non-local term describes how the plastic activity spreads spatially over the system due to non-local elastic relaxation: it accounts for the cooperativity involved in the plastic events occurring during flow, and ξ denotes a bulk 'flow cooperativity length'.

Together with the definition $f(z) = \dot{\gamma}(z)/\sigma(z)$, equation (1) constitutes our non-local rheological model for the emulsion. An analytical solution of equation (1) can be obtained, giving the fluidity at some position z in terms of an integral of the shear stress over the whole channel width. This solution requires two boundary conditions. A first is given by symmetry with respect to the centreline, and $\partial f/\partial z = 0$ at this point. A second boundary condition for the fluidity results from the dynamical behaviour at the surfaces. As we describe in the Supplementary Information, we did characterize the surface flow behaviour by investigating the relationship between wall shear rate and wall shear stress, whose ratio defines the surface fluidity $f_{\mathrm{wall}} = \dot{\gamma}_{\mathrm{wall}}/\sigma_{\mathrm{wall}}$. Interestingly, these measurements demonstrate the existence of a specific surface rheology, $f_{\mathrm{wall}} = f_{\mathrm{wall}}(\dot{\gamma}_{\mathrm{wall}})$, which for a given emulsion is found to depend only on the surface roughness (Supplementary Methods, Supplementary Fig. 7). We note that whatever the boundary condition at the wall, the solution of equation (1) can not reduce to its local form, $f_{\mathrm{bulk}}(z) = f_{\mathrm{bulk}}(\sigma(z))$, owing to the diffusive, non-local term. For convenience we then solved equation (1) numerically with the two above boundary conditions, and

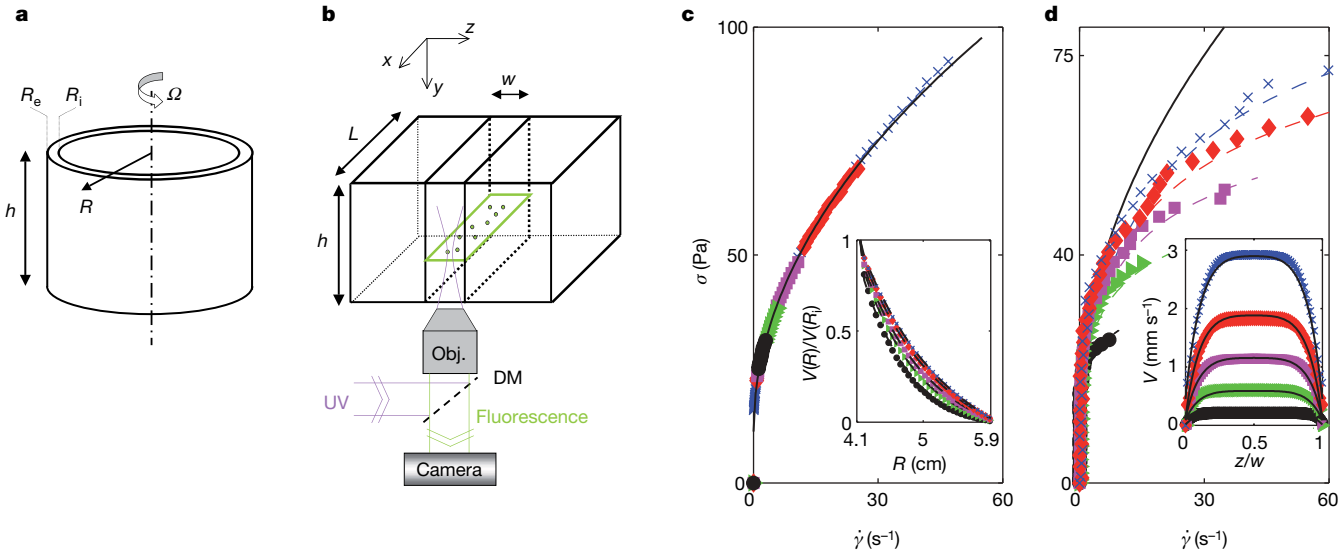

Figure 1 | Local flow curves measured by magnetic resonance imaging and microfluidic velocimetry. **a**, Schematic of the wide gap Couette cell (inner and outer cylinder radii $R_i = 4.1$ cm and $R_e = 5.9$ cm, respectively, gap $w = R_e - R_i = 1.8$ cm, height $h = 11$ cm). **b**, Flow in a microchannel and particle imaging velocimetry. DM, dichroic mirror; UV, ultraviolet lamp; Obj., microscope objective. Flow direction is along x. **c**, **d**, Local flow curves extracted from the measurements of the velocity profiles in both geometries for an emulsion with volume fraction $\phi = 0.75$ and 20% polydispersity. The shear rates are obtained by finite differencing of the velocity profiles given in the insets. Different colours correspond to different rotation velocities (**c**) or different pressure drops (**d**). In **c** are shown local flow curves, $\sigma(z)$ versus $\dot{\gamma}(z)$, extracted from the velocity profiles measured within a wide gap Couette geometry (see inset). The solid line corresponds to the Herschel–Bulkley model with $\sigma_0 = 11.6$ Pa, $A = 11.2$ Pa s$^{1/2}$. Inset, Dimensionless velocity profiles $V(R)/V(R_i)$ as a function of the radial coordinate R. From bottom to top the rotation velocities are 5, 10, 20, 50 and 100 r.p.m. In **d** are shown local flow curves, $\sigma(z)$ versus $\dot{\gamma}(z)$, extracted from the velocity profiles measured in a $w = 250$ μm thick microchannel with rough surfaces, for various pressure drops as a function of the reduced coordinate z/w (see inset). No overlap of the local flow curves is observed. Dashed lines are predictions for the local flow curves at the given ΔP, as obtained from the non-local rheological model of equation (1) with a flow cooperativity length $\xi = 22.3$ μm. The solid line corresponds to the Herschel–Bulkley model with $\sigma_0 = 11.6$ Pa, $A = 11.2$ Pa s$^{1/2}$. Inset, corresponding velocity profiles measured for ΔP equal to 300, 450, 600, 750, 900 mbar. The length of the channel is $L = 14$ cm. Solid lines are the velocity profiles predicted by the non-local rheological model of equation (1). Slippage, which is found to occur at the surfaces as detailed in Supplementary Fig. 7, does not affect the resulting local flow curves as plotted in the main figure.

velocity profiles were deduced by integrating the computed local shear rate $\dot{\gamma}(z)$.

The only remaining parameter is the bulk 'flow cooperativity length' ξ in equation (1). A crucial and surprising finding is that a unique (constant) length ξ accounts for all experimental data for the flow profiles and local flow curves for a given emulsion (Figs 1d and 2), independently of the pressure drop, confinement and surface nature (rough or smooth). That so much data can be fitted using a single and constant length ξ is quite remarkable. Typical comparisons are shown in Figs 1d and 2 for both the velocity profiles and the corresponding local flow curves (see also Supplementary Figs 5 and 6). We mention that alternative non-local rheological models, involving, for example, non-local terms in the flow curve[27], are unable to reproduce all measured flow profiles (Supplementary Fig. 9).

Furthermore, a similar, very good agreement has been obtained for all (jammed) emulsions investigated, with various volume fractions and polydispersities (Supplementary Figs 5 and 6). Figure 3 reports the variation of the measured flow cooperativity length ξ as a function of the volume fraction for emulsions with two different dispersities. Below the jamming concentration $\phi < \phi_c$, we could not measure finite-size effects in the flow profiles within the experimental uncertainty (Supplementary Fig. 3), so that $\xi \approx 0$ in this case. A strong increase of ξ is observed above the jamming threshold, in line with the appearance of elastic and yield properties of the materials in this regime.

Non-local effects in the jammed state are expected to affect the flow behaviour as the cooperativity length ξ is comparable to the confinement width w, that is $\xi/w = \mathcal{O}(1)$. According to equation (1), such confinement effects arise due to fluidity gradients, which may have their origin either in boundary effects or in the existence of gradients of stress occurring at a scale comparable to ξ, that is, $(\nabla\sigma)/\sigma \approx \xi^{-1}$. This is the case for the microfluidic configurations: the orders of magnitude of boundary effects and stress gradients are given by ξ/w, which is indeed up to $\sim$0.5 in this geometry (Figs 1d and 2). On the other hand, for the wide Couette cell (Fig. 1c), boundary effects and stress gradients are much weaker (as estimated by $\xi/w \approx 10^{-3} \ll 1$ and $\xi(\nabla\sigma)/\sigma \approx 2\xi/R_i \approx 10^{-3} \ll 1$). This justifies *a posteriori* the absence of any measured non-local effects in this cell.

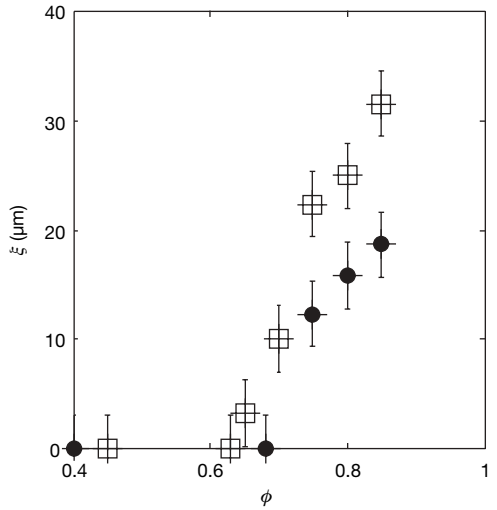

Figure 3 | Flow cooperativity length ξ as a function of emulsion volume fraction ϕ. Squares and circles correspond to emulsions with respective polydispersities of 20% and 36%. The corresponding jamming volume fractions, as determined by the occurrence of a non-vanishing yield stress, are $\phi_c = 0.64$ (squares) and $\phi_c = 0.68$ (circles). Error bars denote the dispersion of the experimental values over various experiments, ± 1 s.d.

Furthermore, as the confinement ratio ξ/w goes to zero, local flow curves increasingly follow the bulk Herschel-Bulkley prediction (Supplementary Fig. 11).

Non-local effects in the flow properties may be *a priori* expected at the microscopic scale[27]. However, we measure a 'flow cooperativity length' only in the jammed state, providing a direct and novel connection between non-local effects and the jamming transition. Furthermore, we emphasize that this length is associated with correlations of a dynamical quantity (the fluidity, that is, rearrangements) and not with static structural order. Typically for the volume fraction range studied here, ξ varies between 0 and 30 μm, compared with the droplet size $d \approx 6$ μm, giving a cooperatively rearranging region involving up to a few hundred particles. These values are close to

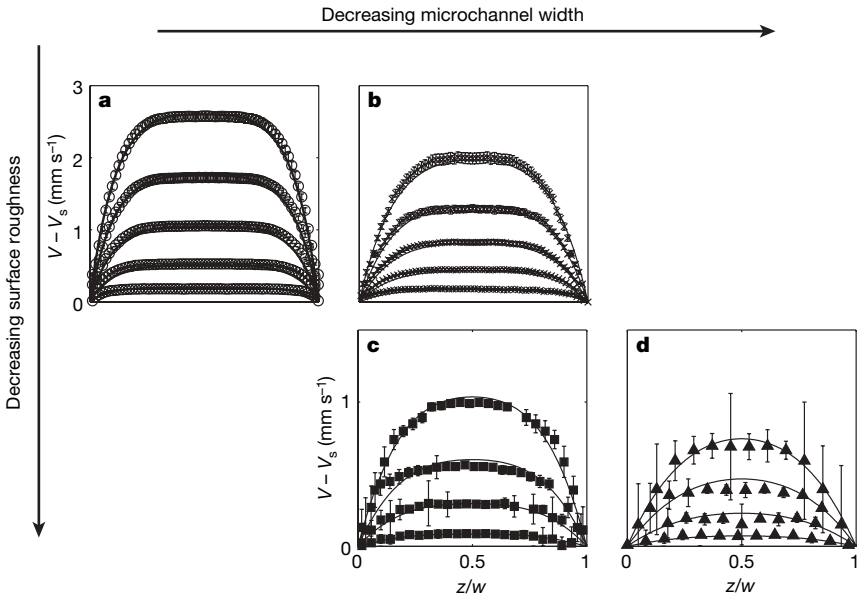

Figure 2 | Velocity profiles in microchannels with different widths w and confining wall roughness, corrected for the slip velocity. **a**, Rough microchannel with $w = 250$ μm; **b**, rough microchannel with $w = 125$ μm; **c**, smooth microchannel with $w = 112$ μm; and **d**, smooth microchannel with $w = 56$ μm. Plotting symbols show data points; solid lines show velocity profiles predicted by the non-local model of equation (1) with a flow cooperativity length $\xi = 22.3$ μm. The various experimental velocity profiles correspond to different pressure drops ΔP, tuned to get the same range of wall shear stress σ_{wall} in the various geometries. From bottom to top in the indicated panels, the values of σ_{wall} (Pa) are: **a**, 27, 41, 55, 68, 82; **b**, 30, 45, 60, 75, 90; **c**, 45, 60, 75, 91; **d**, 48, 65, 82, 97 Pa. The volume fraction is $\phi = 75\%$, with 20% polydispersity. Error bars, $\pm$1s.d. ($n = 450$).

estimates for the dynamical heterogeneities measured in glassy materials[10,11] or in jammed granular materials[14,16,28]. Furthermore, similar observations of non-locality have been reported in granular flows close to the jamming transition[15,29], suggesting further universal characteristics.

However, we emphasize that the present length characterizing flow cooperativity differs fundamentally from that which characterizes dynamical heterogeneities involved in spontaneous fluctuations. Indeed, whereas these dynamical heterogeneities have been measured to exhibit a maximum at the jamming point[10,30], the present flow cooperativity length ξ is non-vanishing in the jammed region only, and increases when going deeper in the jammed phase. This suggests that the flow behaviour of glassy and jammed materials involves physical mechanisms distinct from those associated with the glass transition. We expect that the flow cooperativity length ξ measures the zone of influence of localized plastic events occurring during flow and not the size of mobile regions. Our results thus provide a novel perspective for developing a theoretical framework to describe the non-local flow behaviour of glassy and jammed systems, such as soft glasses and granular materials.

Received 5 November 2007; accepted 18 April 2008.

1. Jop, P., Forterre, Y. & Pouliquen, O. A constitutive law for dense granular flows. *Nature* **441,** 727–730 (2006).
2. Debenedetti, P. G. & Stillinger, F. H. Supercooled liquids and the glass transition. *Nature* **410,** 259–267 (2001).
3. Biroli, G. A new kind of phase transition? *Nature Phys.* **3,** 222–223 (2007).
4. Coussot, P. Rheophysics of pastes: a review of microscopic modelling approaches. *Soft Matter* **3,** 528–540 (2007).
5. Fuchs, M. & Cates, M. E. Theory of nonlinear rheology and yielding of dense colloidal suspensions. *Phys. Rev. Lett.* **89,** 248304 (2002).
6. Goldenberg, C. & Goldhirsch, I. Friction enhances elasticity in granular solids. *Nature* **435,** 188–191 (2005).
7. Ostojic, S., Somfai, E. & Nienhuis, B. Scale invariance and universality of force networks in static granular matter. *Nature* **439,** 828–830 (2006).
8. Liu, A. J. & Nagel, S. R. Jamming is not just cool any more. *Nature* **396,** 21–22 (1998).
9. Berthier, L. Time and length scales in supercooled liquids. *Phys. Rev. E* **69,** 020201(R) (2004).
10. Weeks, E. R., Crocker, J. C., Levitt, A. C., Schofield, A. & Weitz, D. A. Three dimensional direct imaging of structural relaxation near the colloidal glass transition. *Science* **287,** 627–631 (2000).
11. Berthier, L. *et al.* Direct experimental evidence of a growing length scale accompanying the glass transition. *Science* **310,** 1797–1800 (2005).
12. Gao, Y. & Kilfoil, M. L. Direct imaging of dynamical heterogeneities near the colloid-gel transition. *Phys. Rev. Lett.* **99,** 078301 (2007).
13. Priestley, R. D., Ellison, C. L., Broadbelt, L. J. & Torkelson, J. M. Structural relaxation of polymer glasses at surfaces, interfaces and in between. *Science* **309,** 456–459 (2005).
14. Dauchot, O., Marty, G. & Biroli, G. Dynamical heterogeneity close to the jamming transition in a sheared granular material. *Phys. Rev. Lett.* **95,** 265701 (2005).
15. Pouliquen, O. Velocity correlations in dense granular flows. *Phys. Rev. Lett.* **93,** 248001 (2004).
16. Keys, A. S., Abate, A. R., Glotzer, S. C. & Durian, D. J. Measurement of growing dynamical length scales and prediction of the jamming transition in a granular material. *Nature Phys.* **3,** 260–264 (2007).
17. Varnik, F., Bocquet, L., Barrat, J.-L. & Berthier, L. Shear localization in a model glass. *Phys. Rev. Lett.* **90,** 095702 (2003).
18. Leonforte, F., Tanguy, A., Wittmer, J. P. & Barrat, J.-L. Inhomogeneous elastic response of silica glass. *Phys. Rev. Lett.* **97,** 055501 (2006).
19. Isa, L., Besseling, R. & Poon, W. C. Shear zones and wall slip in the capillary flow of concentrated colloidal suspensions. *Phys. Rev. Lett.* **98,** 198305 (2007).
20. Helbing, D., Farkas, I. & Vicsek, T. Simulating dynamical features of escape panic. *Nature* **407,** 487–490 (2000).
21. Degré, G. *et al.* Rheology of complex fluids by particle image velocimetry in microchannels. *Appl. Phys. Lett.* **89,** 024104 (2006).
22. Mueth, D. M. *et al.* Signatures of granular microstructure in dense shear flows. *Nature* **406,** 385–389 (2000).
23. Princen, H. M. Rheology of foams and highly concentrated emulsions. *J. Colloid Interface Sci.* **91,** 160–175 (1983).
24. Schall, P., Weitz, D. A. & Spaepen, F. Structural rearrangements that govern flow in colloidal glasses. *Science* **318,** 1895 (2007).
25. Picard, G., Ajdari, A., Bocquet, L. & Lequeux, F. A simple model for heterogeneous flows of yield stress fluids. *Phys. Rev. E* **66,** 051501 (2002).
26. Picard, G., Ajdari, A., Lequeux, F. & Bocquet, L. Slow flows of yield stress fluids: complex spatiotemporal behavior within a simple elastoplastic model. *Phys. Rev. E* **71,** 010501(R) (2005).
27. Dhont, J. K. G. A constitutive relation describing the shear-banding transition. *Phys. Rev. E* **60,** 4534–4544 (1999).
28. Kamrin, K. & Bazant, M. Z. A stochastic flow rule for granular materials. *Phys. Rev. E* **75,** 041301 (2007).
29. Deboeuf, S., Lajeunesse, E., Dauchot, O. & Andreotti, B. Flow rule, self-channelization and levees in unconfined granular flows. *Phys. Rev. Lett.* **97,** 158303 (2006).
30. Goldman, D. I. & Swinney, H. L. Signatures of glass formation in a fluidized bed of hard spheres. *Phys. Rev. Lett.* **96,** 145702 (2006).

Supplementary Information is linked to the online version of the paper at www.nature.com/nature.

Acknowledgements Discussions with J.-L. Barrat and B. Andreotti are acknowledged. This project was supported by Rhodia, Région Aquitaine and the ANR. L.B. acknowledges support from the von Humboldt Foundation.

Author Information Reprints and permissions information is available at www.nature.com/reprints. Correspondence and requests for materials should be addressed to L.B. (lyderic.bocquet@univ-lyon1.fr) and A.C. (annie.colin-exterieur@eu.rhodia.com).